Materials Horizons

ROYAL SOCIETY OF CHEMISTRY

REVIEW

View Article Online
View Journal | View Issue

Cite this: *Mater. Horiz.*, 2025, **12**, 10414

Perspective on water electrolysis for ozone production: electrocatalyst design and development

Zheng Zhu, Qiangqiang Song, Lili Jiang,* Minmin Yan,* Sheng Chen* and Jingjing Duan*

Received 15th July 2025,
Accepted 27th August 2025

DOI: 10.1039/d5mh01341k

rsc.li/materials-horizons

Electrocatalytic ozone production (EOP) is a new, environmentally friendly, safe and cost-efficient ozone production technology. The slow kinetics and poor stability of conventional catalysts in the EOP process limit its wide application. Consequently, the development and design of novel EOP catalysts are crucial. There have been few reviews on various types of EOP catalysts. Therefore, this paper reviews recent advances on EOP catalysts, categorized by material types. Additionally, the mechanism of EOP is discussed in depth. Finally, we propose constructive implications for future EOP system development. This paper aims to provide an in-depth analysis of the EOP process, summarize and discuss advances in EOP materials, and establish a reliable foundation for future EOP development.

Wider impact

Other than H_2 and O_2, water electrolysis can also be used for producing ozone for versatile applications. But the slow kinetics and poor stability of conventional catalysts for this reaction limit its widespread applications. Thus far, there have been few reviews on various types of ozone production catalysts. Here we report recent developments in ozone production catalysts categorized by material type. Our paper will provide an in-depth understanding of the ozone production process, summarize and discuss advances, and establish a reliable foundation for future development.

Introduction

Electrocatalytic ozone production (EOP) primarily utilizes specific electrocatalysts to generate ozone by oxidizing oxygen molecules in water under an applied electric current. Typically, water serves as the raw material. Oxygen evolution occurs at the anode surface, and when the applied voltage exceeds a certain threshold, a portion of the oxygen molecules undergo further oxidation to produce ozone.[1–6] Under an electric field, the anode-surface electrocatalyst adsorbs water molecules and induces their dissociation into hydroxide ions and protons.[7–12] Hydroxide ions then lose electrons and protons at the anode to form oxygen, while some oxygen molecules adsorb onto active sites where they lose electrons and protons, triggering an oxidation reaction that yields ozone.

EOP possesses several advantages over other ozone production methods: (i) strong oxidizing ability: ozone is a potent oxidizing agent with a redox potential second only to fluorine. It effectively degrades diverse organic pollutants in water, decomposing large organic molecules into smaller fragments, and ultimately mineralizing them to carbon dioxide and water. This confers significant advantages in wastewater treatment and advanced drinking water purification.[13,14] (ii) Tunable selectivity: by adjusting electrode materials, applied potential, and other parameters, the selectivity of the electrocatalytic reaction can be controlled. This enables preferential reaction of ozone with specific pollutants, enhancing treatment efficiency and resource recovery.[15] (iii) Elimination of secondary pollution: this technology utilizes water as the sole feedstock for ozone generation *via* electrocatalysis, requiring no chemical additives. It thereby avoids secondary pollution associated with chemical dosing, aligning with environmental sustainability goals.[13] (iv) Operational simplicity: the EOP system equipment is relatively simple, easy to operate, and easy to automate, reducing labor demand and operating costs. (v) On-site generation: ozone is produced *in situ* within the target water body, eliminating decomposition and leakage risks during storage/transport while improving utilization efficiency and process safety. (vi) Synergistic compatibility: EOP technology integrates effectively with other water treatment processes (*e.g.*, biological treatment and membrane separation), creating synergistic effects that enhance treatment performance, improve effluent quality, and expand application scope in water treatment.[15,16]

Key Laboratory for Soft Chemistry and Functional Materials, School of Energy and Power Engineering, School of Chemistry and Chemical Engineering, Nanjing University of Science and Technology, Ministry of Education, Nanjing 210094, China. E-mail: Jianglili@njust.edu.cn, mm.yan@njust.edu.cn, sheng.chen@njust.edu.cn, jingjing.duan@njust.edu.cn

Nevertheless, EOP also exhibits disadvantages common to electrocatalytic reactions:[17–26] (i) high energy consumption: the EOP process consumes significant electrical energy. This issue becomes particularly pronounced in large-scale applications, potentially increasing operating costs and limiting deployment in energy-constrained or cost-sensitive settings. (ii) Electrode material limitations: while high-performance electrocatalysts are crucial for EOP, efficient materials (*e.g.*, precious metals and their oxides) face high costs and scarcity. Conversely, economical alternatives typically suffer from inadequate catalytic activity and stability, hindering economic viability and large-scale implementation. (iii) Catalyst instability: during operation, electrode-surface catalysts may experience deactivation, poisoning, or corrosion, leading to performance degradation. Regular replacement or regeneration increases operational costs and maintenance requirements. (iv) Constrained ozone yield: compared to traditional ozone generators, EOP technology produces relatively low ozone concentrations. This limitation restricts its applicability for large-scale industrial production or high-concentration ozone demands. (v) Competing side reactions: undesirable reactions (*e.g.*, hydrogen evolution and oxygen reduction) may occur during EOP, reducing current efficiency, compromising ozone production/utilization, and diminishing overall system performance.

In this paper, we review recent advances in EOP systems, encompassing precious metal-based, nonprecious metal-based, toxic metal-based, and nontoxic metal-based materials (Fig. 1a and b). Additionally, we provide an in-depth discussion of the EOP reaction mechanism and propose forward-looking recommendations to address current system limitations.

General mechanism of EOP

Due to the high thermodynamic potential required for EOP, poor catalytic activity under strongly oxidizing conditions, and inherently sluggish reaction kinetics, further complicated by competing oxygen evolution reactions, it is crucial to fundamentally understand the EOP reaction mechanism and investigate catalyst evolution during operation, including active site transformations and deactivation pathways. The general mechanism of EOP is shown in Fig. 1c.

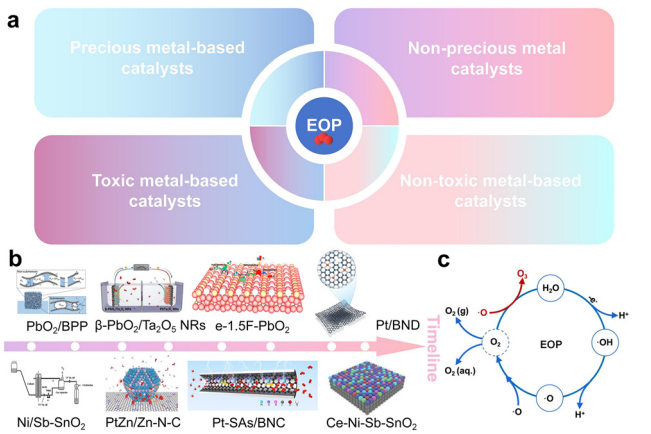

Fig. 1 (a) The schematic diagram of EOP catalyst categorization. (b) A timeline of milestone studies in EOP research.[27–34] (c) The general mechanism of EOP.

Specifically, the anode reaction for aqueous ozone electrolysis proceeds as follows:[35]

$$2H_2O \rightarrow O_2 + 4H^+ + 4e^- \quad E^0 = 1.229\ \text{V } \textit{vs.}\ \text{SHE} \quad (1)$$

$$3H_2O \rightarrow O_3 + 6H^+ + 6e^- \quad E^0 = 1.511\ \text{V } \textit{vs.}\ \text{SHE} \quad (2)$$

$$O_2 + H_2O \rightarrow O_3 + 2H^+ + 2e^- \quad E^0 = 2.075\ \text{V } \textit{vs.}\ \text{SHE} \quad (3)$$

The anodic reaction of water splitting comprises two pathways: the four-electron oxygen evolution reaction (OER) and the six-electron EOP. Similar to the OER, EOP reaction mechanisms involve both the adsorbate evolution mechanism (AEM) and lattice oxygen mechanism (LOM).[36–50]

Adsorbate evolution mechanism

The AEM pathway for EOP follows the sequence: $H_2O \rightarrow OH^* \rightarrow O^* \rightarrow O_2^* \rightarrow O_3^* \rightarrow O_3$. This mechanism primarily involves adsorption/desorption of reactants and intermediates, necessitates a high overpotential to drive the reaction, and is inferred from analogous electrocatalytic reactions like the OER, ORR, *etc.*:[51–58]

$$H_2O \rightarrow OH^* + H^+ + e^- \quad (4)$$

$$OH^* \rightarrow O^* + H^+ + e^- \quad (5)$$

$$2O^* \rightarrow O_2^* \rightarrow O_2 \quad (6)$$

$$O_2^* + O^* \rightarrow O_3^* \rightarrow O_3 \quad (7)$$

Lattice oxygen mechanism

Initially, researchers questioned whether EOP followed a LOM analogous to the classical OER, with no established consensus. The prevailing hypothesis suggested that—conceptually similar to the OER—an EOP LOM pathway would require lattice oxygen participation in ozone-forming steps (*e.g.*, O–O bond formation), rather than relying exclusively on adsorbed oxygen species. This conceptual framework now guides contemporary EOP mechanistic studies. Subsequent research has confirmed LOM in EOP systems, enabling targeted catalyst design.[27,29,35,59–71]

Jiang *et al.* demonstrated the correlation between lattice oxygen activity and the crystal facet structure in β-PbO_2, revealing superior ozone generation efficiency on (110) facets. Their work establishes direct involvement of β-PbO_2 lattice oxygen in electrochemical ozone production, rather than exclusive dependence on surface-adsorbed oxygen species.[72] The enhanced efficiency of (110) facets stems from their higher lattice oxygen activity and favourable electronic structure. Notably, facet-dependent variations in lattice oxygen activation properties govern catalytic activity differences.

EOP catalysts

Synthesis methods

EOP is an efficient and clean method for producing ozone, with its core focus on developing efficient, stable, and economical

anode catalysts. These catalysts must selectively oxidize water molecules to produce ozone rather than oxygen under the competition of the OER. The following is an analysis of some major catalyst types and their typical synthesis methods.

Electrodeposition

Electrodeposition, also known as electroplating or electrolytic deposition, is a method that uses electrochemical principles to deposit a layer of metal, alloy, or compound on the surface of a conductive substrate (cathode), as shown in Fig. 2a. It is a very important surface treatment technology and functional material preparation method. In the EOP system, the most commonly used materials for electrodeposition include β-PbO_2 (orthorhombic crystal system), SnO_2, *etc.*

Pyrolysis

Pyrolysis is one of the most commonly used and important methods for preparing electrocatalysts (especially carbon-based and non-precious metal electrocatalysts). Its core principle involves high-temperature thermal treatment of carbon- and/or metal-containing precursors under inert or specific atmospheres (Fig. 2b). Through thermal decomposition and structural reorganization, this process generates catalytic materials with specific active sites, high specific surface areas, and excellent conductivity.

As with the thermal decomposition synthesis method for the classic EOP material β-PbO_2, a solution containing lead compounds (such as lead acetate) is coated onto a substrate, and high-temperature thermal decomposition oxidation forms a PbO_2 coating. However, the bonding strength and density are typically inferior to those achieved by electroplating. For SnO_2-based catalysts, the method typically involves repeatedly coating (brushing, dipping, and spraying) a mixture of $SnCl_4$ and dopants (such as $SbCl_3$) in hydrochloric acid or alcohol solutions onto a pre-treated titanium substrate. After each coating, the substrate is calcined at high temperatures (400–600 °C) for a certain period of time to decompose and oxidize the precursor into a crystalline SnO_2–Sb_2O_5 (or other doped) coating. This process is repeated multiple times to achieve the desired thickness and density.

Chemical vapor deposition

Chemical vapor deposition (CVD) is an important material preparation technology widely used in the preparation of high-performance thin films, coatings, and nanostructured materials. In the field of electrocatalysts, CVD has attracted widespread attention because it can precisely control the composition, structure, and morphology of catalysts, thereby optimizing their activity, selectivity, and stability. The CVD process involves introducing gaseous precursors (compounds containing the target elements) into a reaction chamber, where chemical reactions (pyrolysis, reduction, oxidation, or synthesis reactions) occur on the surface of a heated substrate, resulting in the deposition of solid products onto the substrate while gaseous byproducts are vented from the system (Fig. 2c).

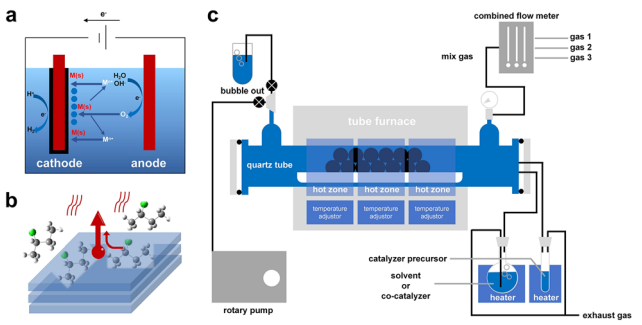

Fig. 2 The schematic diagram of (a) electrodeposition, (b) pyrolysis and (c) chemical vapor deposition.

For example, boron-doped diamond (BDD) has the highest known oxygen evolution overpotential, an extremely wide potential window, exceptional corrosion resistance and chemical inertness, low background current, and can efficiently produce ozone with minimal byproducts under specific conditions, making it an ideal material for high-performance EOP. The general synthesis steps are as follows: in a high-temperature (700–900 °C) and low-pressure reaction chamber, a mixture of gases containing a carbon source (such as methane CH_4), a dopant source (such as borane B_2H_6), and hydrogen is introduced. The carbon source undergoes thermal decomposition on the substrate surface, hydrogen atoms etch away non-diamond carbon, and ultimately a polycrystalline boron-doped diamond thin film is deposited on the substrate surface.

The core of electrocatalytic ozone-producing catalysts lies in anode materials with high oxygen evolution overpotential and high stability. The electrodeposition method for β-PbO_2 is currently the most technically mature and widely applied technique. The CVD method for BDD exhibits excellent performance but comes with extremely high costs. The thermal decomposition method also serves as an important alternative or substrate material. Research on novel catalysts (such as doped modifications, composite structures, and other high overpotential oxides) continues, with synthesis methods primarily based on fundamental chemical techniques like hydrothermal, sol–gel, coprecipitation, and electro-deposition, combined with morphology control and composite technologies. The choice of synthesis method must be determined comprehensively based on the specific material system, performance objectives, cost budget, and process feasibility. In actual research, optimizing synthesis parameters (concentration, temperature, time, current/voltage, doping amount, *etc.*) to achieve optimal performance is of critical importance. In addition, other methods for preparing EOP electrocatalysts are also being developed and applied, such as sol–gel and hydrothermal-assisted electrochemical deposition.

Categories of EOP catalysts

Precious metal-based catalysts. Precious metal-based materials are widely employed in electrocatalysis.[73–79] Among these, platinum (Pt) has been extensively studied for classical reactions (*e.g.*, HER, ORR, OER, *etc.*). While Pt exhibits EOP activity in neutral electrolyte systems, several drawbacks limit its large-scale application: (i) high cost. (ii) Susceptibility to oxidation/dissolution in strongly oxidizing environments, reducing

activity and operational lifetime. (iii) Promotion of competing reactions (*e.g.*, oxygen evolution) during ozone generation, lowering faradaic efficiency. (iv) Surface fouling by impurities or intermediates, decreasing active site availability. (v) Requirement of high overpotentials for effective ozone production, increasing energy consumption. (vi) Environmental impacts from platinum mining/processing and improper catalyst disposal.

Current research addresses these limitations through improving Pt-based catalysts: (i) alloying with other metals to enhance stability and selectivity. (ii) Utilizing high-surface-area supports to improve dispersion. (iii) Engineering nanostructures to increase active sites. (iv) Developing non-precious metal/composite alternatives.

For instance, Gu *et al.* synthesized Pt single atoms embedded in B/N co-doped carbon nanotubes (Pt-SAs/BNC) (Fig. 3a).[32] The Pt-Sas/BNC-3 variant demonstrated exceptional electrochemical activity (Fig. 3b and c) achieving an overpotential of 2.61 V *vs.* RHE at pH 7. This system yielded 4.8 mg L^{-1} dissolved O_3 at 3.0 V (Fig. 3d and e) and 15 mg L^{-1} gaseous O_3 at 50 mA cm^{-2} (Fig. 3f), with a faradaic efficiency of 21% (3.0 V) (Fig. 3g and h) and remarkable 100-hour stability (Fig. 3i). XAFS spectroscopy revealed Pt-Sas/BNC-3's local coordination environment, showing Pt in an oxidation state intermediate between Pt foil and PtO_2 without nanoparticle/cluster formation. The Pt atoms occupy graphene double vacancies coordinated to three pyridinic N atoms and one B atom, conferring enhanced structural stability.

Beyond that example, numerous studies report Pt-based catalysts for EOP applications. Hayashi *et al.* demonstrated a Pt/Ti catalyst achieving 19.7% faradaic efficiency for ozone production,[80] while Mohamed *et al.* developed Pt/TaO_y composites exhibiting high EOP activity (FE = 19.3%),[81] *etc.*

As mentioned above, Pt-based EOP catalyst performance can be significantly improved through alloying, support optimization, nanostructure design, and surface modification, simultaneously reducing costs and enhancing stability. Future research should focus on developing novel composite materials and rational structure designs to advance efficient, economical EOP technology.

Non-precious metal-based catalysts

Non-precious metals offer compelling advantages in electrocatalytic reactions, particularly EOP, due to their low cost, resource sustainability, and environmental friendliness.[82–90] Key benefits include low material cost, earth abundance and minimal environmental impact, tunable multifunctionality, enhanced stability, poisoning resistance, facile modification and optimization, scalable production and high innovation potential. Non-precious metals (*e.g.*, Fe, Co, Ni, Mn, Cu, *etc.*) cost substantially less than precious counterparts (*e.g.*, Pt, Ir, Ru), exhibit high crustal abundance, and require less energy-intensive extraction.[91–98] Their mining/processing reduces ecological disturbance, while end-of-life catalysts enable efficient recycling. Through doping, compositing, or structural engineering, these materials achieve tailored EOP performance while maintaining chemical stability and impurity tolerance under operational conditions.

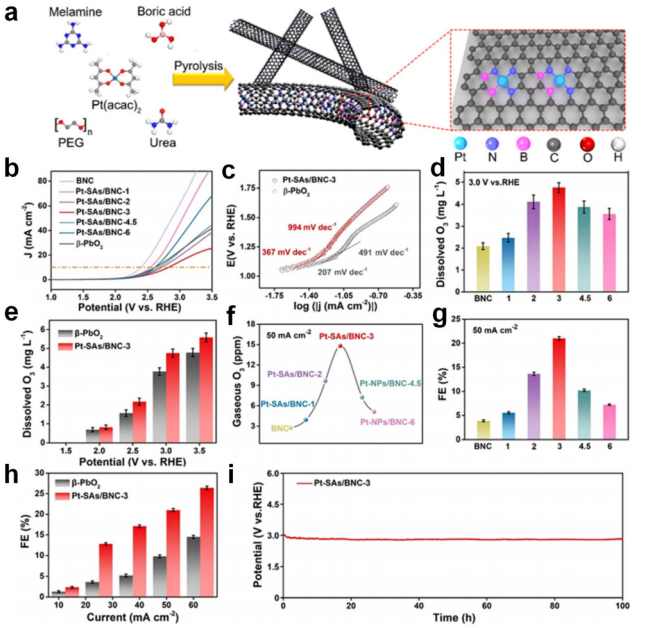

Fig. 3 (a) The synthesis schematic of Pt Sas-BNC; (b) polarization curves; (c) Tafel plot; (d) and I dissolved O_3 field; (f) gaseous O_3 field; (g) and (h) Faraday efficiency of O_3; (i) stability curve. Reproduced from ref. 32 with permission from [American Chemical Society], copyright [2021].

Nickel- and antimony-doped SnO_2 non-precious metal catalysts show excellent potential for electrocatalytic applications. Xue *et al.* synthesized Ce–Ni–Sb–SnO_2 catalysts (Fig. 4a) *via* cerium doping and calcination, achieving exceptional EOP activity.[34] Scanning electron microscopy (SEM), transmission electron microscopy (TEM) and X-ray diffraction (XRD) characterization confirmed successful Ce incorporation and synthesis of Ce–Ni–Sb–SnO_2 (Fig. 4b–f). Among tested formulations, Ce–Ni–Sb–SnO_2 demonstrated optimal electrochemical performance (Fig. 4g–i), yielding 8.0 mg L^{-1} dissolved O_3, 250 mg L^{-1} gaseous O_3 and 43.9% faradaic efficiency at 250 mA cm^{-2} (Fig. 4j–l). Radical quenching experiments (Fig. 4m) elucidated individual radical contributions to efficiency. The system maintained stable operation for 600 h without significant voltage decay (Fig. 4n).

While this study effectively demonstrates non-precious metal applications in EOP, it reveals a significant deviation from conventional performance metrics. Typically, dissolved and gaseous O_3 yields in EOP systems are within the same order of magnitude, differing by no more than several-fold. Remarkably, this work reports an unprecedented gaseous O_3 concentration of 250 mg L^{-1}, exceeding dissolved O_3 levels by 31 times and representing the highest value documented in EOP literature. These exceptional findings suggest that future EOP research should not only build upon existing test protocols but may require innovative measurement approaches and willingness to report and validate extraordinary results that challenge current paradigms.

Toxic metal-based catalysts

Toxic metal-based catalysts, particularly lead (Pb), exhibit enhanced EOP activity but suffer from environmental hazards, poor stability, and undesirable side reactions.[99] During EOP

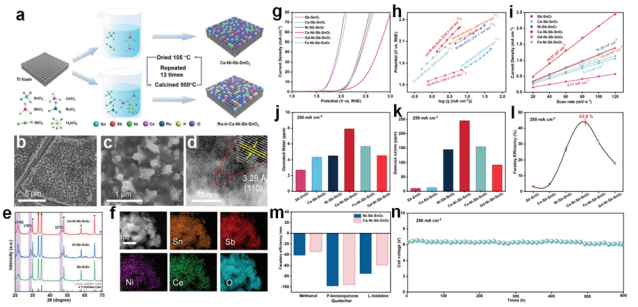

Fig. 4 (a) The synthesis schematic of Ce–Ni–Sb–SnO_2; (b) and (c) SEM images of Ce–Ni–Sb–SnO_2; (d) HRTEM of Ce–Ni–Sb–SnO_2; (e) XRD pattern of Ce–Ni–Sb–SnO_2; (f) elemental mapping of Ce–Ni–Sb–SnO_2; (g) polarization curves; (h) Tafel plot; (i) ECSA plot; (j) dissolved O_3 field; (k) gaseous O_3 field; (l) Faraday efficiency of O_3; (m) effect of free radical quenchers on FE; and (n) stability curve. Reproduced from ref. 34 with permission from [Wiley-VCH], copyright [2023].

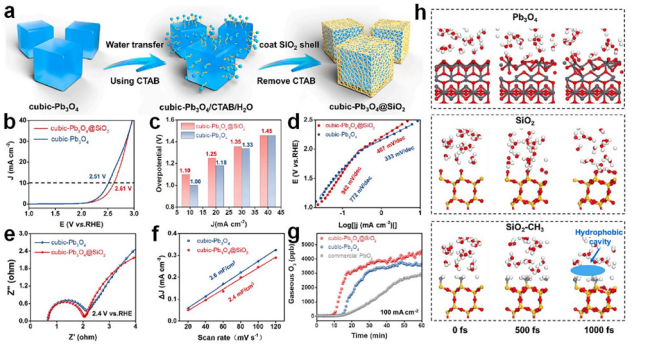

Fig. 5 (a) The synthesis schematic of cubic-Pb_3O_4@SiO_2; (b) polarization curves; (c) overpotential comparison; (d) Tafel plot; (e) EIS plot; (f) ECSA plot; (g) gaseous O_3 field; (h) and structures by AIMD simulations. Reproduced from ref. 100 with permission from [Elsevier B.V.], copyright [2023].

operation, Pb catalysts face critical limitations: (i) potential Pb leaching into aquatic environments causing contamination; (ii) susceptibility to dissolution/corrosion under strong oxidizing conditions; (iii) competing side reactions (*e.g.*, oxygen evolution and metal ion reduction); and (iv) surface poisoning *via* Pb ion adsorption blocking active sites.

Despite numerous reported catalysts with exceptional EOP activity, β-PbO_2 remains the preferred industrial-scale anode material for ozone production due to its optimal balance of catalytic performance, durability and cost-efficient at high current densities. As a classical EOP catalyst, it has been extensively studied for its high anodic oxidation potential, excellent electrical conductivity, and economic viability. However, prolonged operation under harsh oxidative conditions causes dissolution of β-PbO_2 particles, inducing structural degradation that significantly compromises catalytic activity and operational stability.

Owing to the high EOP selectivity of elemental Pb, researchers frequently modify Pb-based catalysts for enhanced performance, exemplified by β-PbO_2's adoption in commercial electrolytic water-based ozone generators. Liu *et al.* synthesized cubic-Pb_3O_4@SiO_2 catalysts through superhydrophobic Pb_3O_4 coating on Si-CH_3-functionalized SiO_2 (Fig. 5a).[100] This material demonstrated exceptional electrochemical activity, yielding 4 mg L^{-1} gaseous O_3, 16.8% faradaic efficiency, and >100 h operational stability with negligible activity decay (Fig. 5b–g). Complementary *ab initio* molecular dynamics (AIMD) simulations elucidated the microscopic origin of cubic-Pb_3O_4@SiO_2's hydrophobicity by modeling three representative configurations (Fig. 5h). By using AIMD simulation to verify surface hydrophobicity, three types of surfaces were compared: Pb_3O_4 (110) (hydrophilic surface), SiO_2 (111) (moderately hydrophilic), and CH_3–SiO_2 (111) (hydrophobic surface). Real water molecule behavior was simulated, and through the evolution of water molecule configuration, surface water layer distance, and radial distribution function, it was analyzed that water molecules on the CH_3–SiO_2 surface formed obvious hydrophobic cavities after 1000 fs, and the water layer separated from the surface. The water molecules on the surface of Pb_3O_4/SiO_2 are tightly adsorbed without the formation of cavities. Hydrophobic cavities provide enrichment space for intermediates, which repel water molecules and reduce the affinity of the electrode surface for water, while enhancing the affinity for gaseous O_2/O_3, promoting ozone generation and diffusion. Experimental and theoretical analyses convergently revealed the fundamental mechanism: Si–CH_3 groups create hydrophobic/oxygen-affinitive microenvironments that enhance active species diffusion at the catalyst-electrolyte interface and oxygen adsorption kinetics—collectively boosting EOP performance.

Numerous additional Pb-based catalysts demonstrate EOP capabilities. For instance, β-PbO_2/Ta_2O_5 achieves a gaseous O_3 yield of 1.65 mg L^{-1} and dissolved an O_3 yield of 2.75 mg L^{-1};[31] PbO_2/bulk porous Pb produces gaseous O_3 at 14 μmol min^{-1} (equivalent to 31.5 mg L^{-1} dissolved O_3);[29] PbO_x-CTAB exhibits 20.7% faradaic efficiency,[101] *etc.* These Pb-containing catalysts show potential to supplant commercial β-PbO_2 while maintaining stable operation at industrial current densities. However, two primary barriers impede their widespread adoption: (i) scalability limitations: current synthesis methods hinder mass production of stabilized catalysts. (ii) Operational instability: structural reconstruction during reaction compromises EOP performance. Therefore, future research should focus on enhancing the stability of Pb-based catalysts by optimizing the structural design and reducing the use of lead to promote the rapid development of efficient and environmentally friendly EOP processes.

Non-toxic metal-based catalysts

The deployment of non-toxic, Pb-free catalysts in EOP holds significant environmental, economic, and sustainability advantages. Through optimized material design and synthesis protocols, these catalysts are poised to drive efficient and eco-friendly ozone production while advancing sustainable electrocatalysis. Among promising Pb-free candidates, MXenes exhibit exceptional EOP applicability due to its high electrical conductivity enabling efficient electron transfer, abundant surface functional groups providing tunable active sites, modifiable

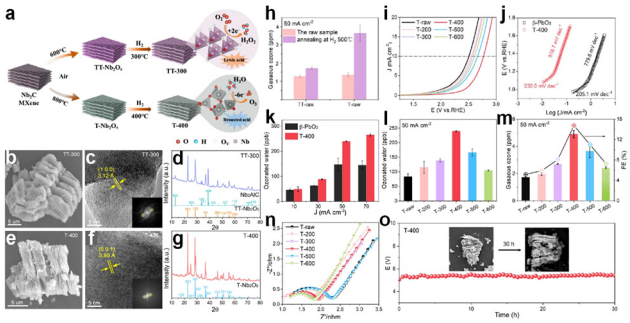

Fig. 6 (a) The synthesis schematic of Nb_2C/Nb_2O_5; (b) and (c) SEM and TEM images of TT-300; (d) XRD pattern of TT-300; (e) and (f) SEM and TEM images of T-400; (g) XRD pattern of T-400; (h) gaseous O_3 field of Nb_2C/Nb_2O_5; (i) LSV curves; (j) Tafel plot; (k) and (l) dissolved O_3 field; (m) FE of gaseous O_3; (n) EIS plot; and (o) stability curve. Reproduced from ref. 104 with permission from [Elsevier B.V.], copyright [2023].

electronic structures *via* compositional engineering, layered architecture with high specific surface area (SSA) maximizing active site exposure and facile synthesis supporting scalable production.[102,103]

For instance, Peng *et al.* designed a series of Nb_2C/Nb_2O_5 catalysts for EOP applications *via* controlled calcination-reduction synthesis (Fig. 6a).[104] The study uniquely integrated two half-reactions, hydrogen peroxide evolution and EOP, for electrochemical synthesis. Comprehensive characterization (including SEM and TEM) confirmed successful fabrication of these MXene composites (Fig. 6b–g). The optimal catalyst (T-400) demonstrated exceptional performance (Fig. 6i, j and n) with a yield of 5 mg L^{-1} for gaseous O_3 (Fig. 6h and m), 0.24 mg L^{-1} for dissolved O_3 (Fig. 6k and l) and robust 30-hour stability in neutral media (Fig. 6o). Mechanistic analysis revealed that oxygen vacancies in T-400 facilitate the formation of an oxygenated OOH* intermediate and enhanced water deprotonation kinetics. This work offers a perspective on the linkages and combinations between electrocatalytic half-reactions.

Beyond classical materials like MXenes, catalysts commonly employed in the ORR, such as ZnO and alloys, have demonstrated applicability in EOP systems.[105–107] This bidirectional catalyst transfer paradigm reveals significant opportunities: EOP materials may be repurposed for other electrocatalytic applications, while established catalysts from related fields can advance EOP technology. Table 1 provides a comparative analysis of recent EOP research literature.

Conclusions and outlook

This review has examined the mechanism of EOP and material systems, yielding the following principal conclusions: (i) Pb-based catalysts remain predominant in industrial EOP applications and (ii) significant potential exists for developing diverse electrocatalyst alternatives.

To address current limitations and future opportunities, we propose:

(i) Advanced *in situ*/operando characterization: the relatively underdeveloped state of EOP research compared to established electrocatalytic reactions (*e.g.*, ORR, OER, HER, and CRR) has limited the application of sophisticated characterization techniques. This gap impedes mechanistic investigation of catalytic processes, preventing deep probing of chemical transformations and reaction pathways. We therefore recommend comprehensive operando analysis to advance fundamental understanding of EOP systems.

(ii) Alkaline EOP system innovation: current EOP research remains confined to acidic and neutral conditions due to rapid ozone decomposition in alkaline media. Realizing full-pH-operable EOP would profoundly advance both mechanistic understanding and industrial implementation. The competitive OER becomes extremely easy and dominant under alkaline conditions, consuming the majority of the current. At the same time, the conversion of key intermediate $^{\bullet}OH$ to $O^{\bullet-}$ weakens the reaction pathway for generating ozone, and the rapid chemical decomposition of ozone in alkali makes it impossible for even trace amounts to accumulate. To overcome the limitations of alkaline EOP, it is necessary to design electrode materials that resist hydroxyl adsorption or develop

Table 1 Comparison of EOP activity between catalysts

Catalyst	pH	O_3^{gas}	$O_3^{dissoved}$	FE	*j*/*V*	Ref.
Pt-SAs/B–N–C	7	15 mg L^{-1}	5.5 mg L^{-1}	26%	50 mA cm^{-2}	32
β-PbO_2/Ta_2O_5	0	1.65 mg L^{-1}	2.75 mg L^{-1}	—	3.5 V	31
PbO_2/bulk porous Pb	0	14 μmol min^{-1}	31.5 mg L^{-1}	—	5 V	29
Ce–Ni–Sb–SnO_2	0	250 mg L^{-1}	8 mg L^{-1}	43.9%	250 mA cm^{-2}	34
e-1.5F-PbO_2	0	95 mg h^{-1} cm^{-2}		14.07%	2.2 A cm^{-2}	33
Pt mesh	7	—	70 wt mg L^{-1}	31%	1.25 A cm^{-2}	108
Pt/TaO_y	7	320 μmol L^{-1}		19.3%	1–2.2 V *vs.* AgCl	81
Pt/Ti	0	33 mg L^{-1}		19.7%	5 V	80
B doped diamond	7	9 mg L^{-1}		40%	2.2 V	109
Ga–Ni–Sb–SnO_2	0	—	0.15 mmol	64%	2.7 V	110
ZnO/ZnS/C	7	2.75 mg L^{-1}	0.5 mg L^{-1}	11%	0.05 A cm^{-2}	105
Nb_2C/Nb_2O_5	7	5 mg L^{-1}	0.24 mg L^{-1}	13%	0.05 A cm^{-2}	104
PbO_x-CTAB-120	7	7 mg L^{-1}	—	20.7%	0.05 A cm^{-2}	101
Cubic-Pb_3O_4@SiO_2	7	4 mg L^{-1}	—	16.8%	0.1 A cm^{-2}	100
$Bi_6Pb_2O_x$	7	11 mg L^{-1}	9 mg L^{-1}	13.5%	0.075 mA cm^{-2}	111
β-PbO_2	7	—	2.12 mg L^{-1}	16.4%	1 A cm^{-2}	112

FE: Faraday efficiency

non-aqueous systems to avoid OH^- interference. The current industrial EOP still relies on acidic systems, and the fundamental reason is the collapse of the lattice oxygen mechanism under alkaline conditions. Consequently, developing effective gas-separation techniques for alkaline environments represents a critical research frontier.

(iii) Pb-free, non-precious catalyst development: while Pb-based systems dominate commercial applications, their environmental toxicity and instability demand alternatives. Similarly, precious metal catalysts face scalability limitations. Hence, the development and design of non-Pb-based and non-precious-metal-based EOP catalysts should not be delayed. Developing Pb-free, non-precious metal EOP catalysts is not only a technical requirement, but also a dual driver of environmental ethics and resource security. Future breakthroughs need to focus on environmentally compatible materials (without heavy metal leaching); rich element high activity design (Fe, Co, and Ni based oxides); and electrode reactor collaborative optimization (such as membrane electrode assembly technology). Only by getting rid of dependence on lead and precious metals can electrocatalytic ozone technology truly achieve green and sustainable applications.

(iv) Next-generation reactor design: conventional electrolyzers dominate current research but suffer from critical limitations, such as prohibitive capital costs, suboptimal structural durability and insufficient operational stability. The improvement of EOP devices can be completed in stages. Primary stage: renovation of the electrolytic cell and optimization of electrodes + addition of pulse power supply + online UV detection. Intermediate stage: building of membrane electrode assembly reactor + split double tank + some control platforms. Advanced stage: development of microfluidic array reactors, combined with AI dynamic regulation. The core of EOP laboratory reactor design is precise control of the ''electro-chemical-mass transfer'' process. Priority should be given to addressing ozone mass transfer limitations and detection reliability, followed by gradual upgrades to non-aqueous phase systems and intelligence. These shortcomings constrain fundamental research and compromise system efficiency. We therefore urge development of advanced reactor architectures.

Conflicts of interest

There are no conflicts to declare.

Data availability

All source data are provided upon request from corresponding authors.

Acknowledgements

The authors would like to acknowledge the financial support from the National Natural Science Foundation (Grant No. 92163124, 52376193 and 52488201), the Jiangsu Natural Science Foundation (Grant No. BK20230097), and the Fundamental Research Funds for the Central Universities (Grant No. 30920041113 and 30921013103).

References

1 T. Y. Dai, T. H. Wang, Z. Wen and Q. Jiang, Recent Progress on Computation-Guided Catalyst Design for Highly Efficient Nitrogen Reduction Reaction, *Adv. Funct. Mater.*, 2024, **34**, 1–20.
2 L. Yang, J. Shui, L. Du, Y. Shao, J. Liu, L. Dai and Z. Hu, Carbon-Based Metal-Free ORR Electrocatalysts for Fuel Cells: Past, Present, and Future, *Adv. Mater.*, 2019, **31**, 1–20.
3 X. Zhao, G. Hu, G. F. Chen, H. Zhang, S. Zhang and H. Wang, Comprehensive Understanding of the Thriving Ambient Electrochemical Nitrogen Reduction Reaction, *Adv. Mater.*, 2021, **33**, 1–46.
4 Z. Zheng, G. Xin, C. Jiayi, C. Ya, C. Xiaodong and L. Cui, Research Progress on Ni-based Electrocatalysts for Electrochemical Reduction of Nitrogen to Ammonia, *Chem. – Eur. J.*, 2024, 202402562.
5 S. B. Patil and D. Y. Wang, Exploration and Investigation of Periodic Elements for Electrocatalytic Nitrogen Reduction, *Small*, 2020, **16**, 1–44.
6 F. Zeng, C. Mebrahtu, L. Liao, A. K. Beine and R. Palkovits, Stability and Deactivation of OER Electrocatalysts: A Review, *J. Energy Chem.*, 2022, **69**, 301–329.
7 K. Zhang and R. Zou, Advanced Transition Metal-Based OER Electrocatalysts: Current Status, Opportunities, and Challenges, *Small*, 2021, **17**, 1–40.
8 S. Li, Y. Wang, Y. Du, X. D. Zhu, J. Gao, Y. C. Zhang and G. Wu, P-Block Metal-Based Electrocatalysts for Nitrogen Reduction to Ammonia: A Minireview, *Small*, 2023, **19**, 1–15.
9 Y. Zi, C. Zhang, J. Zhao, Y. Cheng, J. Yuan and J. Hu, Research Progress in Structure Evolution and Durability Modulation of Ir- and Ru-Based OER Catalysts under Acidic Conditions, *Small*, 2024, 2406657.
10 B. He, F. Bai, P. Jain and T. Li, A Review of Surface Reconstruction and Transformation of 3d Transition-Metal (oxy) Hydroxides and Spinel-Type Oxides during the Oxygen Evolution Reaction, *Small*, 2025, 2411479.
11 J. Wang, J. Kim, S. Choi, H. Wang and J. Lim, A Review of Carbon-Supported Nonprecious Metals as Energy-Related Electrocatalysts, *Small Methods*, 2020, **4**, 1–22.
12 S. Onajah, R. Sarkar, M. S. Islam, M. Lalley, K. Khan, M. Demir, H. N. Abdelhamid and A. A. Farghaly, Silica-Derived Nanostructured Electrode Materials for ORR, OER, HER, CO2RR Electrocatalysis, and Energy Storage Applications: A Review, *Chem. Rec.*, 2024, **24**, e202300234.
13 Q. Zhang, Y. Cao, Y. Yan, B. Yuan, H. Zheng, Y. Gu, X. Zhong and J. Wang, Synergetic Effect of Pyrrolic-N and Doped Boron in Mesoporous Carbon for Electrocatalytic Ozone Production, *J. Mater. Chem. A*, 2020, **8**, 2336–2342.

14 P. A. Christensen, K. Zakaria and T. P. Curtis, Structure and Activity of Ni- and Sb-doped SnO_2 zone Anodes, *Ozone: Sci. Eng.*, 2012, **34**, 49–56.
15 Y.-H. Wang and Q.-Y. Chen, Anodic Materials for Electrocatalytic Ozone Generation, *Int. J. Electrochem.*, 2013, **2013**, 1–7.
16 J. Liu, X. Peng, X. Wang, X. Zhong and J. Wang, Electrochemical Ozone Production: from Fundamental Mechanisms to Advanced Applications, *EES Catal.*, 2025, **3**, 170–204.
17 H. Zhang, Y. Zhang, T. Qiao, S. Hu, J. Liu, R. Zhu, K. Yang, S. Li and L. Zhang, Study on Ultrasonic Enhanced Ozone Oxidation of Cyanide-containing Wastewater, *Sep. Purif. Technol.*, 2022, **303**, 122258.
18 M. Qasim, M. S. Rafique and R. Naz, Water Purification by Ozone Generator Employing Non-thermal Plasma, *Mater. Chem. Phys.*, 2022, **291**, 126442.
19 I. F. Mena, M. A. Montiel, C. Sáez and M. A. Rodrigo, Improving Performance of Proton-exchange Membrane (PEM) Electro-ozonizers Using 3D Printing, *Chem. Eng. J.*, 2023, **464**, 0–7.
20 J. W. Yu, G. Bin Jung, C. W. Chen, C. C. Yeh, X. V. Nguyen, C. C. Ma, C. W. Hsieh and C. L. Lin, Innovative Anode Catalyst Designed to Reduce the Degradation in Ozone Generation via PEM Water Electrolysis, *Renew. Energy*, 2018, **129**, 800–805.
21 C. C. Yang, S. F. Zai, Y. T. Zhou, L. Du and Q. Jiang, Fe_3C-Co Nanoparticles Encapsulated in a Hierarchical Structure of N-Doped Carbon as a Multifunctional Electrocatalyst for ORR, OER, and HER, *Adv. Funct. Mater.*, 2019, **29**, 1–12.
22 J. Quílez-Bermejo, S. García-Dalí, A. Daouli, A. Zitolo, R. L. S. Canevesi, M. Emo, M. T. Izquierdo, M. Badawi, A. Celzard and V. Fierro, Advanced Design of Metal Nanoclusters and Single Atoms Embedded in C_1N_1-Derived Carbon Materials for ORR, HER, and OER, *Adv. Funct. Mater.*, 2023, **33**, 1–12.
23 T. Zhang, B. Zhang, Q. Peng, J. Zhou and Z. Sun, Mo_2B_2M-Bene-supported Single-atom Catalysts as Bifunctional HER/OER and OER/ORR Electrocatalysts, *J. Mater. Chem. A*, 2021, **9**, 433–441.
24 W. Chen, X. Zhu, W. Wei, H. Chen, T. Dong, R. Wang, M. Liu, K. Ostrikov, P. Peng and S. Q. Zang, Neighboring Platinum Atomic Sites Activate Platinum–Cobalt Nanoclusters as High-Performance ORR/OER/HER Electrocatalysts, *Small*, 2023, **19**, 1–12.
25 R. J. Li, W. J. Niu, W. W. Zhao, B. X. Yu, C. Y. Cai, L. Y. Xu and F. M. Wang, Achievements and Challenges in Surfactants-Assisted Synthesis of MOFs-Derived Transition Metal–Nitrogen–Carbon as a Highly Efficient Electrocatalyst for ORR, OER, and HER, *Small*, 2025, **21**, 2408227.
26 M. Jahan, Z. Liu and K. P. Loh, A Graphene Oxide and Copper-Centered Metal Organic Framework Composite as a Tri-Functional Catalyst for HER, OER, and ORR, *Adv. Funct. Mater.*, 2013, **23**, 5363–5372.
27 M. Lu, X. Liu, C. Jing, X. Wang, L. Ding, F. Gao, L. Ren, S. Dai, X. Zhong and J. Wang, Efficient Electrochemical Ozone and Hydrogen Peroxide Production by Synergistic Effect of Atomically Dispersed Pt, Boron and Nitrogen Doped 2D Diamonds, *Adv. Funct. Mater.*, 2024, 2412170.
28 P. A. Christensen, W. F. Lin, H. Christensen, A. Imkum, J. M. Jin, G. Li and C. M. Dyson, Room Temperature, Electrochemical Generation of Ozone with 50% Current Efficiency in 0.5m Sulfuric Acid at Cell Voltages < 3V, *Ozone: Sci. Eng.*, 2009, **31**, 287–293.
29 C. Zhang, Y. Xu, P. Lu, X. Zhang, F. Xu and J. Shi, Capillary Effect-Enabled Water Electrolysis for Enhanced Electrochemical Ozone Production by Using Bulk Porous Electrode, *J. Am. Chem. Soc.*, 2017, **139**, 16620–16629.
30 B. Yuan, Z. Yao, C. Qiu, H. Zheng, Y. Yan, Q. Zhang, X. Sun, Y. Gu, X. Zhong and J. Wang, Synergistic Effect of Size-dependent PtZn Nanoparticles and Zinc Single-atom Sites for Electrochemical Ozone Production in Neutral Media, *J. Energy Chem.*, 2020, **51**, 312–322.
31 Y. Yan, Y. Gao, H. Zheng, B. Yuan, Q. Zhang, Y. Gu, G. Zhuang, Z. Wei, Z. Yao, X. Zhong, X. Li and J. Wang, Simultaneous Electrochemical Ozone Production and Hydrogen Evolution by Using Tantalum-based Nanorods Electrocatalysts, *Appl. Catal., B*, 2020, **266**, 118632.
32 Y. Gu, S. Wang, H. Shi, J. Yang, S. Li, H. Zheng, W. Jiang, J. Liu, X. Zhong and J. Wang, Atomic Pt Embedded in BNC Nanotubes for Enhanced Electrochemical Ozone Production via an Oxygen Intermediate-rich Local Environment, *ACS Catal.*, 2021, **11**, 5438–5451.
33 Q. Yu, Z. Jiang, J. Yin, S. Chen and X. Hu, Unraveling the Role of F in Electrochemical Ozone Generation on the F-Doped PbO_2 Electrode, *J. Phys. Chem. C*, 2022, **126**, 19397–19408.
34 M. Xue, J. Zhao, X. Yu, L. Ding, X. Wang, J. Liu, H. Shi, Y. Xue, Z. Yao, X. Zhong and J. Wang, Facilitating Electrochemical Ozone Production and Chlorine Evolution Reaction by Synergistic Effect of Multicomponent Metal Oxides, *Adv. Funct. Mater.*, 2024, **34**, 1–12.
35 W. Li, G. Feng, J. Liu, X. Zhong, Z. Yao, S. Deng, S. Wang and J. Wang, The Structural and Chemical Reactivity of Lattice Oxygens on β-PbO_2 EOP Electrocatalysts, *Jiegou Huaxue*, 2022, **41**, 2212051–2212059.
36 W. Cheng, Z. P. Wu, D. Luan, S. Q. Zang and X. W. Lou, Synergetic Cobalt-Copper-Based Bimetal–Organic Framework Nanoboxes toward Efficient Electrochemical Oxygen Evolution, *Angew. Chem., Int. Ed.*, 2021, **60**, 26397–26402.
37 K. Ge, S. Sun, Y. Zhao, K. Yang, S. Wang, Z. Zhang, J. Cao, Y. Yang, Y. Zhang, M. Pan and L. Zhu, Facile Synthesis of Two-Dimensional Iron/Cobalt Metal–Organic Framework for Efficient Oxygen Evolution Electrocatalysis, *Angew. Chem., Int. Ed.*, 2021, **60**, 12097–12102.
38 D. Guo, Z. Zeng, Z. Wan, Y. Li, B. Xi, C. Wang, A. CoN-based and O. E. R. Electrocatalyst, Capable in Neutral Medium: Atomic Layer Deposition as Rational Strategy for Fabrication, *Adv. Funct. Mater.*, 2021, **31**, 1–9.
39 T. Wang, P. Wang, W. Zang, X. Li, D. Chen, Z. Kou, S. Mu and J. Wang, Nanoframes of Co_3O_4–Mo_2N Heterointerfaces Enable High-Performance Bifunctionality toward Both

Electrocatalytic HER and OER, *Adv. Funct. Mater.*, 2022, **32**, 1–9.

40 S. Li, M. Yang, Y. Wang, B. Tian, L. Wu, D. Yang, S. Gai and P. Yang, Bridging OER Electrocatalysis and Tumor Therapy: Utilizing Piezoelectric-Hole-Induced OER Electrocatalysis for Direct Oxygen Generation to Address Hypoxia, *Adv. Funct. Mater.*, 2024, 2404169.

41 J. Jia, Y. Wang, Y. Cha, Z. Wang, J. Huang, D. Wang, H. Li, K. Guo, J. Li, J. Huang, Y. Tang and C. Xu, Boosting OER Performance of NiFe-MOFs via Heterostructure Engineering: Promoted Phase Transformation and Self-optimized Dynamic Interface Electron Structure, *Adv. Funct. Mater.*, 2025, 2500568.

42 K. Zhu, X. Zhu and W. Yang, Application of In Situ Techniques for the Characterization of NiFe-Based Oxygen Evolution Reaction (OER) Electrocatalysts, *Angew. Chem., Int. Ed.*, 2019, **58**, 1252–1265.

43 J. Cao, T. Mou, B. Mei, P. Yao, C. Han, X. Gong, P. Song, Z. Jiang, T. Frauenheim, J. Xiao and W. Xu, Improved Electrocatalytic Activity and Stability by Single Iridium Atoms on Iron-based Layered Double Hydroxides for Oxygen Evolution, *Angew. Chem., Int. Ed.*, 2023, **62**, e202310973.

44 A. Malek, Y. Xue and X. Lu, Dynamically Restructuring NixCryO Electrocatalyst for Stable Oxygen Evolution Reaction in Real Seawater, *Angew. Chem., Int. Ed.*, 2023, **62**, e202309854.

45 N. M. Kubo, R. Mhamdi and R. Palkovits, Lanthanum-Nickel-Based Mixed-Oxide-Coated Nickel Electrodes for the OER Electrocatalysis, *Fuel Cells*, 2024, 1–8.

46 J. Saha, S. Verma, R. Ball, C. Subramaniam and R. Murugavel, Compositional Control as the Key for Achieving Highly Efficient OER Electrocatalysis with Cobalt Phosphates Decorated Nanocarbon Florets, *Small*, 2020, **16**, 1–8.

47 H. Yu, J. Ke and Q. Shao, Two Dimensional Ir-Based Catalysts for Acidic OER, *Small*, 2023, **19**, 1–21.

48 F. Zhou, M. Gan, D. Yan, X. Chen and X. Peng, Hydrogen-Rich Pyrolysis from Ni-Fe Heterometallic Schiff Base Centrosymmetric Cluster Facilitates NiFe Alloy for Efficient OER Electrocatalysts, *Small*, 2023, **19**, 1–8.

49 J. Zhu, S. Zi, N. Zhang, Y. Hu, L. An and P. Xi, Surface Reconstruction of Covellite CuS Nanocrystals for Enhanced OER Catalytic Performance in Alkaline Solution, *Small*, 2023, **19**, 1–11.

50 Y. Zhai, X. Ren, J. Zhang, T. Gan, N. Yang, B. Wang and S. Liu, Dynamic Self-Healing of the Reconstructed Phase in Perovskite Oxides for Efficient and Stable Electrocatalytic OER, *Small*, 2024, **2407851**, 1–12.

51 F. Kong, X. Cui, Y. Huang, H. Yao, Y. Chen, H. Tian, G. Meng, C. Chen, Z. Chang and J. Shi, N-Doped Carbon Electrocatalyst: Marked ORR Activity in Acidic Media without the Contribution from Metal Sites?, *Angew. Chem., Int. Ed.*, 2022, **61**, e202116290.

52 X. Li, X. Duan, S. Zhang, C. Wang, K. Hua, Z. Wang, Y. Wu, J. Li and J. Liu, Strategies for Achieving Ultra-Long ORR Durability—Rh Activates Interatomic Interactions in Alloys, *Angew. Chem., Int. Ed.*, 2024, **63**, e202400549.

53 W. Jiao, C. Chen, W. You, J. Zhang, J. Liu and R. Che, Yolk–Shell Fe/Fe_4N@Pd/C Magnetic Nanocomposite as an Efficient Recyclable ORR Electrocatalyst and SERS Substrate, *Small*, 2019, **15**, 1–13.

54 J. Lu, C. Hong, G. Li, X. Zheng, Z. Yin, J. Zhang, Y. Dong, H. Wang, Y. Wang and Y. Deng, Building Cobalt-Nickel Diatomic Sites as Oxygenophilic ORR Catalyst with Strong Cl−-Corrosion Resistance for Seawater Batteries, *Small*, 2024, 2407339.

55 W. Liu, R. Chen, Z. Sang, Z. Li, J. Nie, L. Yin, F. Hou and J. Liang, A Generalized Coordination Engineering Strategy for Single-Atom Catalysts toward Efficient Hydrogen Peroxide Electrosynthesis, *Adv. Mater.*, 2024, 2406403.

56 Y. Zhang, Q. Zhao, B. Danil, W. Xiao and X. Yang, Oxygen-Vacancy-Induced Formation of Pt-Based Intermetallics on MXene with Strong Metal-Support Interactions for Efficient Oxygen Reduction Reaction, *Adv. Mater.*, 2024, **36**, 1–13.

57 A. Vojvodic and J. K. Nørskov, Chemistry: Optimizing Perovskites for the Water-splitting Reaction, *Science*, 2011, **334**, 1355–1356.

58 A. Grimaud, O. Diaz-Morales, B. Han, W. T. Hong, Y. L. Lee, L. Giordano, K. A. Stoerzinger, M. T. M. Koper and Y. Shao-Horn, Activating Lattice Oxygen Redox Reactions in Metal Oxides to Catalyse Oxygen Evolution, *Nat. Chem.*, 2017, **9**, 457–465.

59 T. Binninger, R. Mohamed, K. Waltar, E. Fabbri, P. Levecque, R. Kötz and T. J. Schmidt, Thermodynamic Explanation of the Universal Correlation between Oxygen Evolution Activity and Corrosion of Oxide Catalysts, *Sci. Rep.*, 2015, **5**, 1–7.

60 J. S. Yoo, X. Rong, Y. Liu and A. M. Kolpak, Role of Lattice Oxygen Participation in Understanding Trends in the Oxygen Evolution Reaction on Perovskites, *ACS Catal.*, 2018, **8**, 4628–4636.

61 A. Zagalskaya and V. Alexandrov, Role of Defects in the Interplay between Adsorbate Evolving and Lattice Oxygen Mechanisms of the Oxygen Evolution Reaction in RuO2 and IrO_2, *ACS Catal.*, 2020, **10**, 3650–3657.

62 A. Grimaud, W. T. Hong, Y. Shao-Horn and J. M. Tarascon, Anionic Redox Processes for Electrochemical Devices, *Nat. Mater.*, 2016, **15**, 121–126.

63 J. T. Mefford, X. Rong, A. M. Abakumov, W. G. Hardin, S. Dai, A. M. Kolpak, K. P. Johnston and K. J. Stevenson, Water Electrolysis on $La_{1-x}Sr_xCoO_{3-\delta}$ Perovskite Electrocatalysts, *Nat. Commun.*, 2016, **7**, 11053.

64 F. Y. Chen, Z. Y. Wu, Z. Adler and H. Wang, Stability Challenges of Electrocatalytic Oxygen Evolution Reaction: From Mechanistic Understanding to Reactor Design, *Joule*, 2021, **5**, 1704–1731.

65 J. Suntivich, K. J. May, H. A. Gasteiger, J. B. Goodenough, Y. Shao-Horn and A. Perovskite Oxide, Optimized for Oxygen Evolution Catalysis from Molecular Orbital Principles, *Science*, 2011, **334**, 1383–1385.

66 O. Kasian, S. Geiger, T. Li, J. P. Grote, K. Schweinar, S. Zhang, C. Scheu, D. Raabe, S. Cherevko, B. Gault and K. J. J. Mayrhofer, Degradation of Iridium Oxides via Oxygen Evolution from the Lattice: Correlating Atomic

Scale Structure with Reaction Mechanisms, *Energy Environ. Sci.*, 2019, **12**, 3548–3555.
67 K. A. Stoerzinger, O. Diaz-Morales, M. Kolb, R. R. Rao, R. Frydendal, L. Qiao, X. R. Wang, N. B. Halck, J. Rossmeisl, H. A. Hansen, T. Vegge, I. E. L. Stephens, M. T. M. Koper and Y. Shao-Horn, Orientation-Dependent Oxygen Evolution on RuO_2 without Lattice Exchange, *ACS Energy Lett.*, 2017, **2**, 876–881.
68 K. Klyukin, A. Zagalskaya and V. Alexandrov, Role of Dissolution Intermediates in Promoting Oxygen Evolution Reaction at RuO_2 (110) Surface, *J. Phys. Chem. C*, 2019, **123**, 22151–22157.
69 D. A. Kuznetsov, M. A. Naeem, P. V. Kumar, P. M. Abdala, A. Fedorov and C. R. Müller, Tailoring Lattice Oxygen Binding in Ruthenium Pyrochlores to Enhance Oxygen Evolution Activity, *J. Am. Chem. Soc.*, 2020, **142**, 7883–7888.
70 W. Li, G. Feng, S. Wang, J. Liu, X. Zhong, Z. Yao, S. Deng and J. Wang, Lattice Oxygen of PbO_2 (101) Consuming and Refilling via Electrochemical Ozone Production and H_2O Dissociation, *J. Phys. Chem. C*, 2022, **126**, 8627–8636.
71 X. Rong, J. Parolin and A. M. Kolpak, A Fundamental Relationship between Reaction Mechanism and Stability in Metal Oxide Catalysts for Oxygen Evolution, *ACS Catal.*, 2016, **6**, 1153–1158.
72 W. Jiang, S. Wang, J. Liu, H. Zheng, Y. Gu, W. Li, H. Shi, S. Li, X. Zhong and J. Wang, Lattice Oxygen of PbO_2 Induces Crystal Facet Dependent Electrochemical Ozone Production, *J. Mater. Chem. A*, 2021, **9**, 9010–9017.
73 V. R. Stamenkovic, B. S. Mun, M. Arenz, K. J. J. Mayrhofer, C. A. Lucas, G. Wang, P. N. Ross and N. M. Markovic, Trends in Electrocatalysis on Extended and Nanoscale Pt-bimetallic Alloy Surfaces, *Nat. Mater.*, 2007, **6**, 241–247.
74 C. Zhang, Y. Cui, Y. Yang, L. Lu, S. Yu, Z. Meng, Y. Wu, Y. Li, Y. Wang, H. Tian and W. Zheng, Highly Conductive Amorphous Pentlandite Anchored with Ultrafine Platinum Nanoparticles for Efficient pH-Universal Hydrogen Evolution Reaction, *Adv. Funct. Mater.*, 2021, **31**, 1–11.
75 F. Lin, Z. Dong, Y. Yao, L. Yang, F. Fang and L. Jiao, Electrocatalytic Hydrogen Evolution of Ultrathin Co-Mo_5N_6 Heterojunction with Interfacial Electron Redistribution, *Adv. Energy Mater.*, 2020, **10**, 1–7.
76 L. B. Huang, L. Zhao, Y. Zhang, Y. Y. Chen, Q. H. Zhang, H. Luo, X. Zhang, T. Tang, L. Gu and J. S. Hu, Self-Limited on-Site Conversion of MoO_3 Nanodots into Vertically Aligned Ultrasmall Monolayer MoS_2 for Efficient Hydrogen Evolution, *Adv. Energy Mater.*, 2018, **8**, 1–7.
77 H. Liu, Q. Liu, Y. Shao, R. Wang, M. Cheng, J. Hu, T. Wei, B. Liu, H. Jiang, L. Qi, M. Chen, W. Lu, W. Li and X. Li, Single-Atom Nickel Encapsulated in Nanosheet-Coiled rGO-CTAB-MoS_2 Nanoflowers for High-Efficiency and Long-Term Hydrogen Evolution in Acidic Medium, *Adv. Funct. Mater.*, 2025, 2425826.
78 A. Chandran M, P. Dutta, P. Singh, A. K. Singh and B. L. V. Prasad, Design and Synthesis of PtPdNiCoMn High-Entropy Alloy Electrocatalyst for Enhanced Alkaline Hydrogen Evolution Reaction: A Theoretically Supported Predictive Design Approach, *Adv. Funct. Mater.*, 2024, 2418644.
79 Y. Q. Zhou, L. Zhang, H. L. Suo, W. Hua, S. Indris, Y. Lei, W. H. Lai, Y. X. Wang, Z. Hu, H. K. Liu, S. L. Chou and S. X. Dou, Atomic Cobalt Vacancy-Cluster Enabling Optimized Electronic Structure for Efficient Water Splitting, *Adv. Funct. Mater.*, 2021, **31**, 1–8.
80 M. Hayashi, T. Ochiai, S. Tago, H. Saito, T. Yahagi and A. Fujishima, Electrolytic Ozone Generation at Pt/Ti Electrode Prepared by Multiple Electrostrike Method, *Chem. Lett.*, 2019, **48**, 574–577.
81 M. I. Awad, S. Sata, K. Kaneda, M. Ikematsu and T. Ohsaka, Ozone Electrogeneration on Pt-TaOy Sol-gel Film Modified Titanium Electrode: Effect of Electrode Composition on the Electrocatalytic Activity, *J. Energy Chem.*, 2015, **24**, 178–184.
82 W. Yu, H. Huang, Y. Qin, D. Zhang, Y. Zhang, K. Liu, Y. Zhang, J. Lai and L. Wang, The Synergistic Effect of Pyrrolic-N and Pyridinic-N with Pt Under Strong Metal-Support Interaction to Achieve High-Performance Alkaline Hydrogen Evolution, *Adv. Energy Mater.*, 2022, **12**, 1–8.
83 F. Zhu, S. Li, X. Bu, J. Ge, W. L. Song, M. Wang and S. Jiao, Sustainable Processing of Ultralow-Cost Petroleum Cokes Into Ultrastable Self-Doped Fe_3C@CNT Catalysts for High-Efficiency HER, *Small*, 2024, 2407502.
84 C. Saetta, I. Barlocco, G. Di Liberto and G. Pacchioni, Key Ingredients for the Screening of Single Atom Catalysts for the Hydrogen Evolution Reaction: The Case of Titanium Nitride, *Small*, 2024, 2401058.
85 Q. Li, F. Huang, S. Li, H. Zhang and X. Y. Yu, Oxygen Vacancy Engineering Synergistic with Surface Hydrophilicity Modification of Hollow Ru Doped CoNi-LDH Nanotube Arrays for Boosting Hydrogen Evolution, *Small*, 2022, **18**, 1–11.
86 Y. K. Li, G. Zhang, H. Huang, W. T. Lu, F. F. Cao and Z. G. Shao, $Ni_{17}W_3$–W Interconnected Hybrid Prepared by Atmosphere- and Thermal-Induced Phase Separation for Efficient Electrocatalysis of Alkaline Hydrogen Evolution, *Small*, 2020, **16**, 1–10.
87 Y. Guan, Y. Feng, J. Wan, X. Yang, L. Fang, X. Gu, R. Liu, Z. Huang, J. Li, J. Luo, C. Li and Y. Wang, Hydrogen Evolution Reaction: Ganoderma-Like MoS_2/NiS_2 with Single Platinum Atoms Doping as an Efficient and Stable Hydrogen Evolution Reaction Catalyst, *Small*, 2018, **14**, 1870125.
88 P. Liu, X. Zhang, J. Fei, Y. Shi, J. Zhu, D. Zhang, L. Zhao, L. Wang and J. Lai, Frank Partial Dislocations in Coplanar Ir/C Ultrathin Nanosheets Boost Hydrogen Evolution Reaction, *Adv. Mater.*, 2024, **36**, 1–8.
89 Q. Li, C. Chen, W. Luo, X. Yu, Z. Chang, F. Kong, L. Zhu, Y. Huang, H. Tian, X. Cui and J. Shi, In Situ Active Site Refreshing of Electro-Catalytic Materials for Ultra-Durable Hydrogen Evolution at Elevated Current Density, *Adv. Energy Mater.*, 2024, **14**, 1–11.
90 V. Jose, V. H. Do, P. Prabhu, C. K. Peng, S. Y. Chen, Y. Zhou, Y. G. Lin and J. M. Lee, Activating Amorphous

Ru Metallenes Through Co Integration for Enhanced Water Electrolysis, *Adv. Energy Mater.*, 2023, **13**, 1–13.

91 A. Li, Q. Cao, G. Zhou, B. V. K. J. Schmidt, W. Zhu, X. Yuan, H. Huo, J. Gong and M. Antonietti, Three-Phase Photocatalysis for the Enhanced Selectivity and Activity of CO_2 Reduction on a Hydrophobic Surface, *Angew. Chem., Int. Ed.*, 2019, **58**, 14549–14555.

92 S. Y. Chae, J. Y. Choi, Y. Kim, D. Le Tri Nguyen and O. S. Joo, Photoelectrochemical CO_2 Reduction with a Rhenium Organometallic Redox Mediator at Semiconductor/Aqueous Liquid Junction Interfaces, *Angew. Chem., Int. Ed.*, 2019, **58**, 16395–16399.

93 Z. Ma, T. Zhang, L. Lin, A. Han and J. Liu, Ni Single-atom Arrays as Self-supported Electrocatalysts for CO_2RR, *AIChE J.*, 2023, **69**, 1–8.

94 T. S. Bui, E. C. Lovell, R. Daiyan and R. Amal, Defective Metal Oxides: Lessons from CO_2RR and Applications in NO_xRR, *Adv. Mater.*, 2023, **35**, 2205814.

95 L. Xiong, X. Zhang, L. Chen, Z. Deng, S. Han, Y. Chen, J. Zhong, H. Sun, Y. Lian, B. Yang, X. Yuan, H. Yu, Y. Liu, X. Yang, J. Guo, M. H. Rümmeli, Y. Jiao and Y. Peng, Geometric Modulation of Local CO Flux in Ag@Cu_2O Nanoreactors for Steering the CO_2RR Pathway toward High-Efficacy Methane Production, *Adv. Mater.*, 2021, **33**, 1–11.

96 M. Sun, H. H. Wong, T. Wu, Q. Lu, L. Lu, C. H. Chan, B. Chen, A. W. Dougherty and B. Huang, Double-Dependence Correlations in Graphdiyne-Supported Atomic Catalysts to Promote CO_2RR toward the Generation of C_2 Products, *Adv. Energy Mater.*, 2023, **13**, 1–16.

97 H. Shi, L. Luo, C. Li, Y. Li, T. Zhang, Z. Liu, J. Cui, L. Gu, L. Zhang, Y. Hu, H. Li and C. Li, Stabilizing Cu^+ Species in Cu_2O/CuO Catalyst via Carbon Intermediate Confinement for Selective CO_2RR, *Adv. Funct. Mater.*, 2024, **34**, 1–7.

98 S. Li, J. Yu, S. Zhang, W. Qiu, X. Tang, Z. Lin, R. Cai, Y. Fang, S. Yang and X. Cai, Operando Reconstruction of Porous Carbon Supported Copper Selenide Promotes the C_2 Production from CO_2RR, *Adv. Funct. Mater.*, 2024, **34**, 1–9.

99 V. Naresh, L. Elias, S. A. Gaffoor and S. K. Martha, Corrosion Resistant Polypyrrole Coated Lead-Alloy Positive Grids for Advanced Lead-Acid Batteries, *J. Electrochem. Soc.*, 2019, **166**, A74–A81.

100 J. Liu, C. Qiu, Z. Xu, M. Xue, J. Cai, H. Shi, L. Ding, X. Li, X. Zhong and J. Wang, Tailoring Hydrophobic-aerophilic Microenvironment for Robust Electrochemical Ozone Production, *Chem. Eng. J.*, 2023, **468**, 143504.

101 J. Liu, S. Wang, J. Cai, L. Wu, Y. Liu, J. He, Z. Xu, X. Peng, X. Zhong, L. An and J. Wang, Synergistic Promotion by Highly Active Square-shaped Lead Oxide and Visualized Electrolyzer for Enhanced Electrochemical Ozone Production, *Chin. J. Catal.*, 2024, **57**, 80–95.

102 C. Tsounis, P. V. Kumar, H. Masood, R. P. Kulkarni, G. S. Gautam, C. R. Müller, R. Amal and D. A. Kuznetsov, Advancing MXene Electrocatalysts for Energy Conversion Reactions: Surface, Stoichiometry, and Stability, *Angew. Chem., Int. Ed.*, 2023, **62**, e202210828.

103 J. Chen, Q. Long, K. Xiao, T. Ouyang, N. Li, S. Ye and Z. Q. Liu, Vertically-interlaced NiFeP/MXene Electrocatalyst with Tunable Electronic Structure for High-efficiency Oxygen Evolution Reaction, *Sci. Bull.*, 2021, **66**, 1063–1072.

104 X. Peng, Z. Bao, S. Zhang, Y. Li, L. Ding, H. Shi, J. Liu, X. Zhong, X. Li and J. Wang, Modulation of Lewis and Brønsted Acid Centers with Oxygen Vacancies for Nb_2O_5 Electrocatalysts: Towards Highly Efficient Simultaneously Electrochemical Ozone and Hydrogen Peroxide Production, *Chem. Eng. Sci.*, 2023, **271**, 118573.

105 L. Ding, J. Zhao, Z. Bao, S. Zhang, H. Shi, J. Liu, G. Wang, X. Peng, X. Zhong and J. Wang, Synchronous Generation of Green Oxidants H_2O_2 and O_3 by Using a Heterojunction Bifunctional ZnO/ZnS@C Electrocatalyst, *J. Mater. Chem. A*, 2023, **11**, 3454–3463.

106 F. Gao, X. Li, L. Liu, M. Lu, H. Shi, X. Yu, L. Ding, S. Wang, S. Dai, X. Zhong and J. Wang, Effective Electrochemical Ozone Production Coupled with Hydrogen Evolution Reaction by Synergistic Effect of PtCo Alloy and Borides, *Chem. Eng. Sci.*, 2025, **309**, 121444.

107 C. Wang, Y. Yang, Y. Yuan, Q. Lv, L. Zhou, L. Wang, X. Zheng, J. Liu, H. Wu, D. Pang and J. Zheng, Applications, Performance Enhancement Strategies and Prospects of NixPy in Electrocatalysis, *Mater. Horiz.*, 2025, **12**, 2840–2877.

108 F. Okada, S. Tanaka, S. Tanaka and K. Naya, Electrochemical Production of 70 wt ppm Ozone Water, *Electrochim. Acta*, 2015, **153**, 210–216.

109 Y. Honda, T. A. Ivandini, T. Watanabe, K. Murata and Y. Einaga, An Electrolyte-free System for Ozone Generation Using Heavily Boron-doped Diamond Electrodes, *Diam. Relat. Mater.*, 2013, **40**, 7–11.

110 J. L. Lansing, L. Zhao, T. Siboonruang, N. H. Attanayake, A. B. Leo, P. Fatouros, S. M. Park, K. R. Graham, J. A. Keith and M. Tang, Gd-Ni-Sb-SnO_2 Electrocatalysts for Active and Selective Ozone Production, *AIChE J.*, 2021, **67**, e17486.

111 H. Shi, G. Feng, T. Sun, X. Wang, L. Ding, Z. Wang, H. Jin, Q. Chen, S. Wang, X. Zhong, Y. Zhu and J. Wang, Convex Polyhedral Nanocrystals with High-index and Low-index Microfacets for Electrochemical Co-production of Ozone and Hydrogen Peroxide, *Chem. Catal.*, 2023, **3**, 100728.

112 J. Liu, S. Wang, Z. Yang, C. Dai, G. Feng, B. Wu, W. Li, L. Shu, K. Elouarzaki, X. Hu, X. Li, H. Wang, Z. Wang, X. Zhong, Z. J. Xu and J. Wang, Phase Shuttling-enhanced Electrochemical Ozone Production, *EES Catal.*, 2023, **1**, 301–311.

